ISBN: 978-3-95450-191-5 doi:10.18429/JACoW-SRF2017-THPB025

A CRYSTAL PLASTICITY STUDY ON INFLUENCE OF DISLOCATION MEAN FREE PATH ON STAGE II HARDENING IN Nb SINGLE CRYSTALS

T. Maiti, A. Chakraborty, P. Eisenlohr, D. Kang, and T.R. Bieler
Chemical Engineering and Materials Science
Michigan State University, East Lansing, MI 48824, USA

Abstract

Constitutive models based on thermally-activated stress-assisted dislocation kinetics have been successful in predicting deformation behavior of crystalline materials, particularly in face-centered cubic (fcc) metals. In body-centered cubic (bcc) metals, success has been more or less limited, owing to the ill-defined nature of slip planes and non-planar spreading of $1/2\langle 1\,1\,1\rangle$ screw dislocation cores. As a direct consequence of this, bcc metals show a strong dependence of flow stress on temperature and strain rate, and violation of Schmid law. We present high-resolution full-field crystal plasticity simulations of single crystal Niobium under tensile loading with an emphasis on multi-stage hardening, orientation dependence, and non-Schmid behavior. A dislocation density-based constitutive model with storage and recovery rates derived from Discrete Dislocation Dynamics is used to model strain hardening in stage II. The influence of dislocation mean free path and initial dislocation content on stage II hardening is simulated and compared with in-situ tensile experiments.

INTRODUCTION

When processing pure niobium into superconducting radio-frequency (SRF) cavities, the inherent deformation anisotropy of the individual grains leads to variability in the final cavity properties [1]. Deformation paths involving surface working, such as spinning, introduce gradients of deformation from the surface inward, with a higher density of defects near the surface. To gain precise control of a forming process, it is essential to understand the mesoscopic deformation behavior in terms of stresses necessary to activate dislocation slip on various slip systems and the work hardening behavior resulting from dislocation interactions. Identification of these criteria is important for predicting how crystal orientations and flow stresses will evolve in more complex forming operations.

Single crystal tensile deformation along four exemplary crystallographic directions illustrated in Fig. 1 exhibits a large variability in strain hardening. Capturing such multi-stage hardening with existing phenomenological constitutive descriptions, such as proposed by [2, 3], has seen limited success. In the present work, a constitutive model with dislocation storage and recovery rates based on Discrete Dislocation Dynamics is used to model strain hardening in stage II. Adjustable parameters in this model are identified based on an inverse strategy that uses a Nelder–Mead simplex approach to minimize the deviation between measured and simulated uniaxial single crystal tension experiments.

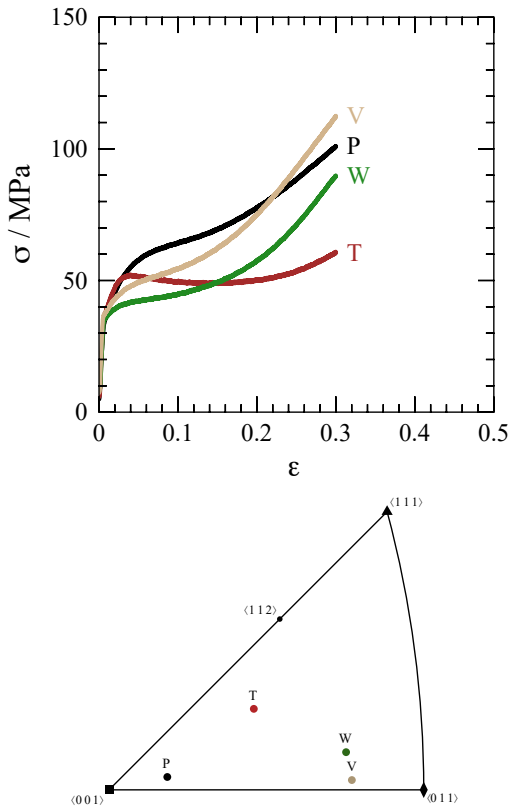

Figure 1: Strong orientation dependence of single crystal strain hardening in Nb ($\dot{\epsilon} \approx 10^{-3}\,\mathrm{s}^{-1}$ at room temperature) [4].

METHODS

Continuum Mechanics

A finite strain framework is adopted in which the total deformation gradient $\mathbf{F} = \mathbf{F}_\mathrm{e}\mathbf{F}_\mathrm{p}$ at each material point is multiplicatively decomposed into elastic $\mathbf{F}_\mathrm{e}$ and plastic $\mathbf{F}_\mathrm{p}$ components, thus introducing an intermediate (or 'lattice') configuration. The second Piola–Kirchhoff stress $\mathbf{S} = \mathbb{C} : \left(\mathbf{F}_\mathrm{e}{}^\mathrm{T}\mathbf{F}_\mathrm{e}\right)/2 = f\left(\dot{\mathbf{F}}, \boldsymbol{\eta}\right)$ reflects the elastic lattice distortion ($\mathbb{C}$ being the fourth-order elastic stiffness tensor) and drives the plastic velocity gradient $\mathbf{L}_\mathrm{p}(\mathbf{S}, \boldsymbol{\eta}) = \dot{\mathbf{F}}_\mathrm{p}\,\mathbf{F}_\mathrm{p}{}^{-1}$ as well as the evolution of internal state variables $\boldsymbol{\eta}$ (see [5] for details).

ISBN: 978-3-95450-191-5 doi:10.18429/JACoW-SRF2017-THPB025

Crystal Plasticity

The microstructural state of the material is defined by the dislocation densities ϱ^{ξ} on twelve $\langle 1\,1\,1\rangle\{1\,1\,0\}$ and twelve $\langle 1\,1\,1\rangle\{1\,1\,2\}$ slip systems indexed by $\xi = 1, \ldots, 24$.

The dislocation kinetics is based on an additively composed resistance to dislocation motion $s^{\xi} = s^{\xi}_{\text{ath}} + s^{\xi}_{\text{th}}$ with an athermal part considering the different interaction strength between dislocation families [6]

$$s^{\xi}_{\text{ath}} = \mu b \sqrt{\sum_{\beta} A_{\xi\beta}\, \varrho^{\beta}} \tag{1}$$

(isotropic shear modulus μ, Burgers vector length b and dimensionless dislocation interaction coefficients $A_{\xi\beta}$ between slip systems ξ and β established using Discrete Dislocation Dynamics (DDD) calculations [7]) and a thermal part s_{th} that accounts for the Peierls potential and solute strengthening. Thermal activation results in a temperature-dependent shear rate

$$\dot{\gamma}^{\xi} = \varrho^{\xi} b v_0 \exp\left\{\frac{-\Delta G_0}{k_{\text{B}} T}\left[1 - \left(\frac{\left|\tau^{\xi} - s^{\xi}_{\text{ath}}\right|}{s^{\xi}_{\text{th}}}\right)^{p}\right]^{q}\right\} \tag{2}$$

(Boltzmann constant k_{B}, absolute temperature T, reference dislocation velocity v_0, parameters p and q describe the shape of the thermal obstacle with free energy ΔG_0 [8], and resolved stress τ).

The elastic interactions of dislocation segments gliding in multiple slip planes lead to formation of dislocation junctions responsible for increased strain hardening in stage II. Dislocation storage and recovery is assumed to be connected to a strain increment $\mathrm{d}\gamma^{\xi}$ by

$$d\varrho^{\xi} = \frac{1}{b}\left(\frac{s^{\xi}_{\text{ath}}}{\mu b K_{hkl}} - y_{hkl}\,\varrho^{\xi}\right)\left|d\gamma^{\xi}\right| \tag{3}$$

with orientation-dependent K_{hkl} and y_{hkl} being a dislocation mean free path coefficient and a distance governing spontaneous dislocation annihilation, respectively [9].

Table 1 lists the values of all constitutive parameters that are fixed and, therefore, not part of the optimization.

Inverse Identification Scheme

Figure 2 explains the identification strategy for inversely obtaining the adjustable constitutive parameters. The optimization module ("optimizer") constitutes a general Python class featuring different stochastic and deterministic optimization algorithms such as Particle Swarm Optimization [10] and Nelder–Mead simplex [11], which for the present study was slightly modified [12] to recover from potential non-convergence of a crystal plasticity simulation. The implemented optimization class can be subclassed with an arbitrary objective function, which in the present case is obtained by considering the absolute deviation $\epsilon_{\text{tension}}$ between the measured and simulated single crystal stress–strain response upon uniaxial tension normalized by the overall deformation work. The simulation of uniaxial deformation used the spectral solver included in the open-source Düsseldorf Advanced Materials Simulation Kit (DAMASK), [13]. An overall $4 \times 4 \times 4$ cubic grid with a central $2 \times 2 \times 4$ volume reflecting the Nb single crystal and the surrounding being made up of a soft, dilatational, and low-stiffness material to mimic the boundary conditions of two free lateral surfaces that otherwise are lost owing to the intrinsically periodic geometry.

Table 1: Constitutive Material Parameters of Pure Nb Used for the Crystal Plasticity Simulations of Uniaxial Tension

Parameter	Value
C_{11}	246.5 GPa
C_{12}	134.5 GPa
C_{44}	28.73 GPa
μ	39.6 GPa
b	0.33 nm
v_0	10^{-4} m s^{-1}
ΔG_0	2.72×10^{-19} J
T	300 K
s_{th}	8.5 MPa
p	0.85
q	1.27
K_{hkl}	
y_{hkl}	
$\varrho_0^{\{1\,1\,0\}}$	
$\varrho_0^{\{1\,1\,2\}}$	

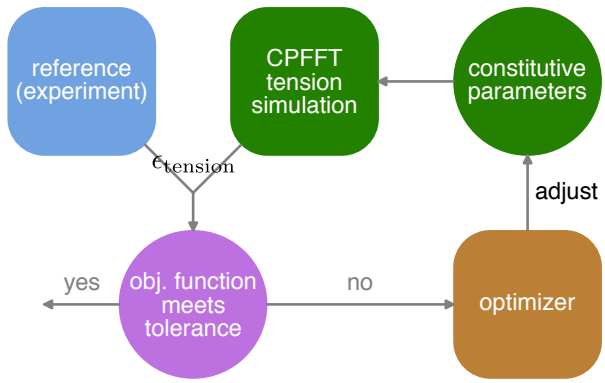

Figure 2: Schematic representation of the inverse identification strategy for crystal plasticity constitutive parameters. Based on the selected optimization algorithm the "optimizer" adjusts the constitutive parameters to be used as input for simulating the uniaxial tension experiment. Crystal plasticity fast Fourier transform (CPFFT) simulation is then performed using DAMASK and the deviation $\epsilon_{\text{tension}}$ between the measured and simulated stress–strain response serves as the objective function.

ISBN: 978-3-95450-191-5 doi:10.18429/JACoW-SRF2017-THPB025

RESULTS AND DISCUSSION

Figure 3 shows the uniaxial stress–strain response resulting after optimization of K_{hkl}, y_{hkl}, and the initial dislocation content $\varrho_0^{\{1\,1\,0\}}$ and $\varrho_0^{\{1\,1\,2\}}$. The experimentally observed variability associated with the different crystallographic tension directions is closely reproduced. Except for orientation 'P', the stage II hardening, which starts to become apparent at strain levels of around 0.2, is generally well captured.

Table 2 presents the underlying values of the adjustable parameters for all four orientations.

Table 2: Variability in Constitutive Parameter Values Resulting From Minimizing the Deviation in Single Crystal Stress–Strain Response for Four Distinct Tensile Directions

Orientation	K_{hkl}	y_{hkl} (nm)	$\varrho_0^{\{1\,1\,0\}}$ (10^{12} m^{-2})	$\varrho_0^{\{1\,1\,2\}}$ (10^{12} m^{-2})
P	20.00	4.29	0.62	0.12
T	15.52	5.52	0.83	0.15
W	5.56	4.56	0.12	0.07
V	7.16	7.16	0.08	0.07

The annihilation distance y_{hkl}, which is governing the dynamic dislocation recovery, is not strongly dependent on the specific orientation, but assumes values of around 5 nm each. This invariance is understandable as the dislocation density accumulated during the straining is still noticeably below that density for which Eq. (3) would reach a dynamic equilibrium, hence, would show a strong influence of the dynamic recovery aspect.

The dislocation storage parameter K_{hkl} exhibits a notably stronger dependence on the crystallographic tensile direction. As such, the simplified model employed here is of limited use for general application in which complex (i.e. not only unidirectional) loadings can occur. Therefore, as a future step, the modeling of dislocation storage needs to take into account the instantaneous dislocation densities to more directly capture the kinematics and dynamics of dislocation junction formation as was already indicated by [9].

The values of initial[1] dislocation density ($\varrho_0^{\{1\,1\,0\}}$ and $\varrho_0^{\{1\,1\,2\}}$ that are necessary to match the yield stress level in each of the four single crystal experiments also exhibit an appreciable variability. Since it is close to impossible to accurately determine the true dislocation content in the material, a numerical study was performed to gauge the influence of this uncertainty on the predicted single crystal stress–strain response in unidirectional tension. Figure 4 presents for the exemplary orientation 'V' that even for a known (fixed) total initial dislocation content, if distributed unevenly across the individual slip systems, the resulting strain hardening can markedly differ. In the case shown, three of the realizations did not even exhibit the experimentally observed

[1] homogeneously distributed across each of the twelve slip systems per slip family

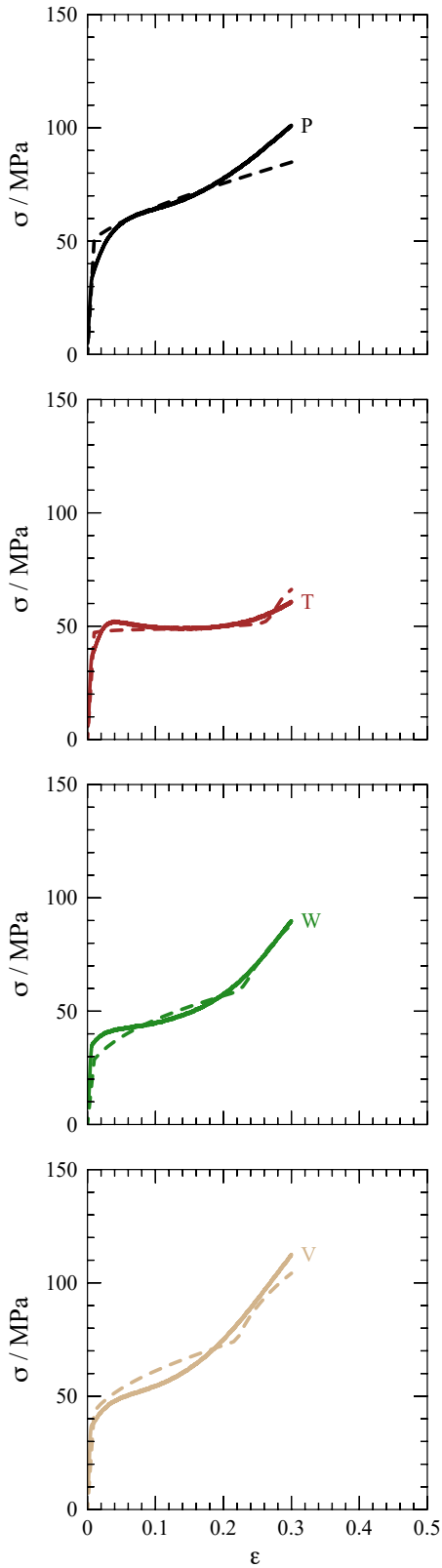

Figure 3: Comparison of experimentally observed (solid) and predicted (dashed) uniaxial stress–strain response for different orientations (see Fig. 1). The coefficients for mean free path K_{hkl} and dynamic recovery y_{hkl} in the model by [9] were estimated using inverse optimization of the measured stress–strain curves.

ISBN: 978-3-95450-191-5 doi:10.18429/JACoW-SRF2017-THPB025

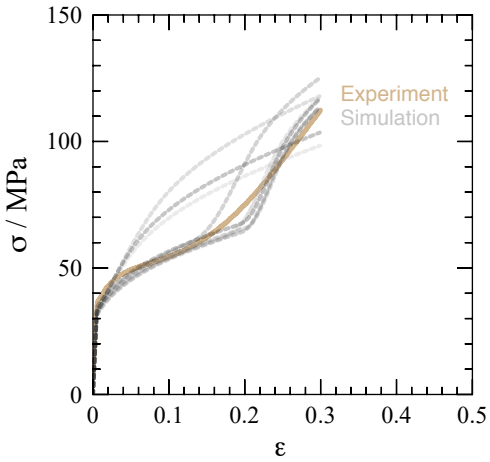

Figure 4: Variability in predicted single–crystal response under unidirectional tension due to different distributions among the slip systems for fixed total initial dislocation content.

two-stage hardening, indicating that the precise matching of single crystal deformation is likely elusive even with rather elaborate constitutive models.

ACKNOWLEDGMENTS

Financial support from the Department of Energy through grant DE-SC0009962 and the National Science Foundation through grant DMR-1411102 is gratefully acknowledged. This work was supported in part by Michigan State University through computational resources provided by the Institute for Cyber-Enabled Research (iCER).

REFERENCES

[1] T. R. Bieler, D. Kang, D. C. Baars, S. Chandrasekaran, A. Mapar, G. Ciovati, N. T. Wright, F. Pourboghrat, J. E. Murphy, C. C. Compton, and G. R. Myneni, "Deformation mechanisms, defects, heat treatment, and thermal conductivity in large grain niobium," in *AIP Conference Proceedings*, vol. 1687, 2015, p. 020002.

[2] A. Mapar, H. Ghassemi-Armaki, F. Pourboghrat, and K. S. Kumar, "A differential-exponential hardening law for non-Schmid crystal plasticity finite element modeling of ferrite single crystals," *International Journal of Plasticity*, vol. 91, pp. 268–299, 2017.

[3] J. L. Bassani and T.-Y. Wu, "Latent Hardening in Single Crystals II. Analytical Characterization and Predictions," *Proceedings of the Royal Society A: Mathematical, Physical and Engineering Sciences*, vol. 435, no. 1893, pp. 21–41, 1991.

[4] T. R. Bieler, N. T. Wright, F. Pourboghrat, C. Compton, K. T. Hartwig, D. Baars, A. Zamiri, S. Chandrasekaran, P. Darbandi, H. Jiang, E. Skoug, S. Balachandran, G. E. Ice, and W. Liu, "Physical and mechanical metallurgy of high purity Nb for accelerator cavities," *Physical Review Special Topics – Accelerators and Beams*, vol. 13, no. 3, p. 031002, 2010.

[5] F. Roters, P. Eisenlohr, L. Hantcherli, D. D. Tjahjanto, T. R. Bieler, and D. Raabe, "Overview of constitutive laws, kinematics, homogenization, and multiscale methods in crystal plasticity finite element modeling: Theory, experiments, applications," *Acta Materialia*, vol. 58, pp. 1152–1211, 2010.

[6] P. Franciosi, M. Berveiller, and A. Zaoui, "Latent hardening in copper and aluminium single crystals," *Acta Metallurgica*, vol. 28, no. 3, pp. 273–283, 1980.

[7] R. Madec and L. P. Kubin, "Dislocation strengthening in FCC metals and in BCC metals at high temperatures," *Acta Materialia*, vol. 126, pp. 166–173, 2017.

[8] U. F. Kocks, A. S. Argon, and M. F. Ashby, "Thermodynamics and Kinetics of Slip," *Progress in Materials Science*, vol. 19, pp. 1–291, 1975.

[9] B. Devincre, T. Hoc, and L. Kubin, "Dislocation Mean Free Paths and Strain Hardening of Crystals," *Science*, vol. 320, no. 5884, pp. 1745–1748, 2008.

[10] J. Kennedy and R. Eberhart, "Particle swarm optimization," in *Proceedings of IEEE International Conference on Neural Networks IV*, 1995, pp. 1942–1948.

[11] J. A. Nelder and R. Mead, "A Simplex Method for Function Minimization," *The Computer Journal*, vol. 7, no. 4, pp. 308–313, 1965.

[12] A. Chakraborty and P. Eisenlohr, "Evaluation of an inverse methodology for estimating constitutive parameters in face-centered cubic materials from single crystal indentations," *European Journal of Mechanics / A Solids*, vol. 66C, pp. 114–124, 2017.

[13] F. Roters, P. Eisenlohr, C. Kords, D. D. Tjahjanto, M. Diehl, and D. Raabe, "DAMASK: The Düsseldorf Advanced Material Simulation Kit for studying crystal plasticity using an FE based or a spectral numerical solver," in *Procedia IUTAM: IUTAM Symposium on Linking Scales in Computation: From Microstructure to Macroscale Properties*, O. Cazacu, Ed., vol. 3. Amsterdam: Elsevier, 2012, pp. 3–10.